















Reconciling Top-Down and Bottom-Up Estimates of Ecosystem Respiration in a Mature Eucalypt Forest

†Deceased

N. J. Noh¹ , A. A. Renchon^{2,3,4} , J. Knauer^{2,5} , V. Haverd^{5†}, J. Li⁶ , A. Griebel^{2,7} ,
C. V. M. Barton² , J. Yang² , D. Sihi⁸ , S. K. Arndt⁹ , E. A. Davidson¹⁰ ,
M. G. Tjoelker² , and E. Pendall² 

Key Points:

- Concurrent scaled chamber measurements matched flux tower observations to within 10%
- Implementing a substrate function into a land surface model improved representation of heterotrophic respiration
- Discrepancies between observations and simulations were largest for temperature sensitivity of canopy and root respiration

Supporting Information:

Supporting Information may be found in the online version of this article.

Correspondence to:

E. Pendall,
e.pendall@westernsydney.edu.au

Citation:

Noh, N. J., Renchon, A. A., Knauer, J., Haverd, V., Li, J., Griebel, A., et al. (2024). Reconciling top-down and bottom-up estimates of ecosystem respiration in a mature eucalypt forest. *Journal of Geophysical Research: Biogeosciences*, 129, e2024JG008064. <https://doi.org/10.1029/2024JG008064>

Received 4 FEB 2024

Accepted 23 SEP 2024

Author Contributions:

Conceptualization: N. J. Noh, E. A. Davidson, E. Pendall
Data curation: N. J. Noh, A. A. Renchon, J. Knauer, V. Haverd, A. Griebel, J. Yang
Formal analysis: N. J. Noh, A. A. Renchon, J. Knauer
Funding acquisition: S. K. Arndt, M. G. Tjoelker, E. Pendall
Investigation: N. J. Noh, J. Li, J. Yang
Methodology: N. J. Noh, J. Knauer, C. V. M. Barton, J. Yang, D. Sihi
Project administration: E. Pendall
Resources: E. Pendall

¹Division of Forest Science, College of Forest and Environmental Science, Kangwon National University, Chuncheon, South Korea, ²Hawkesbury Institute for the Environment, Western Sydney University, Penrith, NSW, Australia, ³Division of Geological and Planetary Sciences, California Institute of Technology, Pasadena, CA, USA, ⁴Environmental Science Division, Argonne National Laboratory, Lemont, IL, USA, ⁵CSIRO Environment, Canberra, ACT, Australia, ⁶Ministry of Education Key Laboratory for Biodiversity Science and Ecological Engineering, School of Life Sciences, Fudan University, Shanghai, China, ⁷School of Life Sciences, University of Technology Sydney, Broadway, NSW, Australia, ⁸Department of Plant & Microbial Biology and Crop and Soil Sciences, North Carolina State University, Raleigh, NC, USA, ⁹School of Ecosystem and Forest Sciences, The University of Melbourne, Richmond, VIC, Australia, ¹⁰Appalachian Laboratory, University of Maryland Center for Environmental Science, Frostburg, MD, USA

Abstract Ecosystem respiration (R_{eco}) arises from interacting autotrophic and heterotrophic processes constrained by distinct drivers. Here, we evaluated up-scaling of observed components of R_{eco} in a mature eucalypt forest in southeast Australia and assessed whether a land surface model adequately represented all the fluxes and their seasonal temperature responses. We measured respiration from soil (R_{soil}), heterotrophic soil microbes (R_{h}), roots (R_{root}), and stems (R_{stem}) in 2018–2019. R_{eco} and its components were simulated using the CABLE-POP (Community Atmosphere-Biosphere Land Exchange–Population Orders Physiology) land surface model, constrained by eddy covariance and chamber measurements and enabled with a newly implemented Dual Arrhenius and Michaelis-Menten (DAMM) module for soil organic matter decomposition. Eddy-covariance based R_{eco} ($R_{\text{eco,eddy}}$, $1,439 \text{ g C m}^{-2} \text{ y}^{-1}$) was slightly higher than the sum of the respiration components ($R_{\text{eco,sum}}$, $1,295 \text{ g C m}^{-2} \text{ y}^{-1}$) and simulated R_{eco} ($1,297 \text{ g C m}^{-2} \text{ y}^{-1}$). The largest mean contribution to R_{eco} was from R_{soil} (64%) across seasons. The measured contributions of R_{h} (49%), R_{root} (15%), and R_{stem} (22%) to $R_{\text{eco,sum}}$ were very close to model outputs of 46%, 11%, and 22%, respectively. The modeled R_{h} was highly correlated with measured R_{h} ($R^2 = 0.66$, $\text{RMSE} = 0.61$), empirically validating the DAMM module. The apparent temperature sensitivities (Q_{10}) of R_{eco} were 2.22 for $R_{\text{eco,sum}}$, 2.15 for $R_{\text{eco,eddy}}$, and 1.57 for CABLE-POP. This research demonstrated that bottom-up respiration component measurements can be successfully scaled to eddy covariance-based R_{eco} and help to better constrain the magnitude of individual respiration components as well as their temperature sensitivities in land surface models.

Plain Language Summary Ecosystem respiration (R_{eco}) represents losses of carbon from the land to the atmosphere and consists of aboveground plant respiration and belowground root and microbial respiration. Because respiration processes increase exponentially with temperature, understanding their contributions to R_{eco} is critical to predicting carbon cycle responses to warming. We used field observations to test and improve the modeling of respiration components of an evergreen eucalypt forest in Australia. Field measurements indicated that the model adequately captured the quantitative contributions of respiration components to R_{eco} . In particular, the improved microbial version of the model was in good agreement with measurements. However, improvements are needed for modeling and measuring the autotrophic components from roots, stems, and forest canopy. This study highlights that scaling up individual respiratory sources and their temperature responses provides insights to understanding ecosystem scale carbon cycle-climate feedbacks.

1. Introduction

Ecosystem respiration (R_{eco}), the second largest carbon flux between the biosphere and the atmosphere after gross primary productivity, plays a critical role in the response of terrestrial ecosystems to changing climate (Friedlingstein et al., 2023; IPCC, 2022; Zhang et al., 2021). R_{eco} is the sum of autotrophic respiration by plants (R_{a}), often partitioned into leaf, stem, and root components, and heterotrophic respiration by micro-organisms (R_{h}). Each of these components responds differently to environmental drivers and thus to global change factors

© 2024. The Author(s).

This is an open access article under the terms of the [Creative Commons Attribution-NonCommercial-NoDerivs License](https://creativecommons.org/licenses/by/4.0/), which permits use and distribution in any medium, provided the original work is properly cited, the use is non-commercial and no modifications or adaptations are made.

Software: V. Haverd
Supervision: E. Pendall
Validation: J. Knauer
Visualization: N. J. Noh, A. A. Renchon
Writing – original draft: N. J. Noh, J. Knauer, E. Pendall
Writing – review & editing: N. J. Noh, A. A. Renchon, J. Knauer, J. Li, A. Griebel, C. V. M. Barton, J. Yang, D. Sihi, S. K. Arndt, E. A. Davidson, M. G. Tjoelker, E. Pendall

(Loveys et al., 2003; Trumbore, 2006; Wang et al., 2014). Soil, air, and plant surface temperature affect the different components of R_a , while soil biophysical environment (temperature and moisture) and soil carbon substrate availability primarily affect R_h (Davidson et al., 2006; Sihi et al., 2018). Measuring R_{eco} concurrently and its components can improve our understanding of the controlling factors and thus reduce uncertainties in modeled predictions of future ecosystem carbon cycling and functioning (Carbone et al., 2016; Oikawa et al., 2017; Phillips et al., 2017).

The contributions of respiratory components to R_{eco} vary across temporal and spatial scales differently depending on environmental drivers and plant phenological patterns (Brændholt et al., 2018). In particular, temperature sensitivity, which can be defined with several metrics, is commonly used in respiration models (Johnston et al., 2021). In a mature eucalypt forest, we recently demonstrated unrealistically high apparent thermal response of R_{eco} compared to soil respiration (R_{soil}) (Renchon et al., 2021) suggesting that the aboveground components such as leaf respiration (R_{leaf}) may respond more sensitively to temperature changes in the study site than belowground components. However, a meta-analysis demonstrated that R_h can have a stronger and more sustained response to warming than R_a (Wang et al., 2014) but it has also been shown that presence of roots increases temperature sensitivity of R_{soil} (Li et al., 2020). Clearly, temperature sensitivities of respiration differ among components: leaves and roots across several ecosystems (Loveys et al., 2003); roots and microbes in a temperate forest (Noh et al., 2017); stems (Noh et al., 2021), roots, and soil in various forest ecosystems (Wang et al., 2006); leaves, stems, and soil in subtropical forests (Chi et al., 2020); and roots, mycorrhizal hyphae, and microbes in a temperate forest (Makita et al., 2021). These differences suggest that more concurrent measurements of respiratory components and related mechanisms of temperature sensitivity are needed to improve modeling of R_{eco} dynamics and future climate (Liu et al., 2022; Qubaja et al., 2020; Renchon et al., 2021; Sun et al., 2023).

Several techniques are used to estimate R_{eco} in forest ecosystems, but often they do not agree, contributing to uncertainties in global carbon cycle models (Wang et al., 2017). The most widely used method is the direct top-down estimation by the eddy covariance technique which measures net ecosystem exchange (NEE) as the sum of vertical turbulent flux and change in storage in a control volume (Aubinet et al., 2012; Baldocchi, 2014). Eddy covariance R_{eco} ($R_{eco,eddy}$) can then be derived from NEE using flux partitioning algorithms (Isaac et al., 2017; Tramontana et al., 2020). In addition, R_{eco} can be estimated by bottom-up approaches ($R_{eco,sum}$) as a sum of chamber-based measurements of multiple respiratory components that have been scaled-up to the ecosystem level (Law et al., 1999; Wang et al., 2017). Although labor-intensive and prone to sampling biases in space and time, chamber methods have an advantage over the eddy covariance technique because of their ability to distinguish CO_2 emissions from components such as soil, foliage, and woody tissue (Barba et al., 2018). Moreover, common problems and biases for eddy covariance partitioning occur when turbulence is insufficient (Aubinet et al., 2012) and when simple temperature functions such as Q_{10} (a parameter of the temperature sensitivity by which respiration rate increases with a $10^\circ C$ increase in temperature) are used to extrapolate from nighttime to daytime (Wohlfahrt & Galvagno, 2017). These empirical challenges contribute to a longstanding mismatch between up-scaled $R_{eco,sum}$ and top-down $R_{eco,eddy}$ that has yet to be resolved (Phillips et al., 2017; Speckman et al., 2015; Wang et al., 2017). Therefore, chamber-based measurements are essential to estimate the contribution and uncertainty of each component flux to the overall R_{eco} and can be insightful for validating eddy covariance data and models (Liu et al., 2022; Qubaja et al., 2020; Renchon et al., 2021; Wang et al., 2017).

A recent analysis demonstrated that modeled R_{eco} rates were significantly more uncertain than eddy covariance observations and that the estimated temperature sensitivity was lower in the models than observations (Sun et al., 2023). Robust predictions of terrestrial carbon-climate feedbacks require new research to address these uncertainties and biases at various scales. The Community Atmosphere-Biosphere Land Exchange model–Population Orders Physiology (CABLE-POP, Haverd et al., 2018) is a land surface model that can be applied at site or ecosystem scales and is used for global simulations that contribute to the annual global carbon budget assessment (Friedlingstein et al., 2023). All respiration components in the model are temperature dependent on daily timescales and R_a acclimates to seasonal changes in growth temperature (Aspinwall et al., 2016; Atkin et al., 2015; Haverd et al., 2018). The default model version uses standard empirical relationships to represent the effects of soil temperature and moisture on R_h . However, the response of R_h to temperature relies in part also on variations in substrate availability (Davidson & Janssens, 2006). Therefore, we implemented the Dual Arrhenius Michaelis-Menten (DAMM) framework (Davidson et al., 2012) into CABLE-POP which accounts for the combined effects of substrate, temperature, and moisture on R_h . DAMM improved estimates of decomposition fluxes in moisture-limited forests in the northeastern US (Sihi et al., 2018), informed soil CO_2 efflux estimates in a

eucalypt forest exposed to elevated CO₂ (Drake et al., 2018), and enhanced the validity of warming effects on soil carbon when incorporated into the Terrestrial Ecosystem Model (Hao et al., 2015).

In this study, we evaluated the scaling of bottom-up (chamber-based) and top-down (eddy covariance-based) estimates of respiratory CO₂ fluxes in a warm-temperate eucalyptus forest in southeast Australia, the Cumberland Plain near Sydney. We measured the seasonal variability in R_{eco} and its components using automatic chambers and eddy covariance techniques and compared the measurements with simulations using an improved version of CABLE-POP that includes soil organic matter decomposition fluxes via the DAMM model. We aimed to quantify the apparent temperature sensitivities and the contribution of each observed respiration component to total R_{eco} in order to reduce uncertainties and improve the modeled representation of respiratory processes from components to ecosystem scales.

2. Materials and Methods

2.1. Site Description

This study was conducted in the Cumberland Plain forest where the EucFACE and flux tower sites are located (latitude -33.6152 , longitude 150.7236 , 23 m above sea level), near Sydney, Australia. Ecosystem component respiration rates were measured at the EucFACE study site, within the same patch of mature dry sclerophyll forest, ~ 1.4 km from the flux tower (Renchon et al., 2021). The flux site is a Terrestrial Ecosystem Research Network (TERN) OzFlux SuperSite (Fluxnet code: AU-Cum). The plant community of the study sites has remained unmanaged for at least the past 90 years (Jiang et al., 2020) and undisturbed by fire in >20 years (Renchon et al., 2021). The tree canopy was dominated by *Eucalyptus tereticornis* Sm.; stand density varied between 600 and 1,000 trees ha⁻¹ with trees ranging from 18 to 23 m tall and mean diameter at breast height of 18.8 ± 0.6 cm (S.E.) (Noh et al., 2021). The understory vegetation consisted of a subcanopy dominated by *Melaleuca decora* (Salisb.) ex Britten, a shrub layer dominated by *Bursaria spinosa* Cav. and *Breynia oblongifolia* Müll.Arg., and ground cover of grasses and forbs. Standing aboveground biomass at both sites was $\sim 4,700$ g C m⁻², and total net primary production was about 600 g C m⁻² yr⁻¹ averaged across 2014–2017 (Renchon et al., 2021).

The mean (1994–2021) annual temperature was 17.7°C and mean annual precipitation was 741.1 mm (Bureau of Meteorology, station 067105 in Richmond, NSW Australia, <http://www.bom.gov.au>). During the study period (2018–2019), the temperature was higher than average (18.6°C in 2018 and 18.7°C in 2019) while the precipitation was below average with 524 mm in 2018 and 514 mm in 2019.

2.2. Flux Measurements

2.2.1. Measurements of R_{soil}, R_h, and R_{root}

Measurement methods and abbreviations are summarized in Table S1 of the Supporting Information S1 for reference. We measured half-hourly CO₂ fluxes from soil surface (R_{soil}) using three automated CO₂ flux measurement systems (LI-8100A infrared gas analyzers, LI-COR Environmental, Lincoln, NE, USA) each coupled to an automated soil respiration chamber of 20 cm diameter (Li-8100-103) at three different ambient plots (rings) at EucFACE ($n = 3$, separated by >200 m) (Drake et al., 2018). The raw data were quality controlled with a threshold criterion of coefficient of variation (<0.13) and coefficient of determination of the fit ($R^2 > 0.97$). We retained 52%, 54%, and 61% of potential data from chamber one to chamber three, respectively, due to mechanical interruptions or quality control checks. We gapfilled the data from each of the three chambers individually using the semi-mechanistic Dual Arrhenius and Michaelis-Menten kinetics (DAMM) model (Davidson et al., 2012; Renchon et al., 2021) and averaged the three independent chamber time-series to produce a continuous data set of R_{soil}.

Soil heterotrophic respiration (R_h) was measured near the LI-8100 auto-chambers using three forced diffusion (FD) chambers (Eosense eosFD, Dartmouth, Nova Scotia, Canada) (Figure S1 in Supporting Information S1). Root exclusion involved excavating soil pits by horizon to 45-cm depth, removing roots, and replacing root-free soil and the intact litter layer into PVC pipe (20-cm diameter) in January 2018. Data were collected every 30 min for 18 months from February 2018 to August 2019. We only used the R_h data starting 7 months after root exclusion treatment to avoid disturbance artifacts. The three chambers collected 89%, 96%, and 92% of the study period. Flux data were removed when malfunction events were flagged by the eosFD software (e.g., power

outages, negative values as measurement errors). Root respiration was estimated as the difference between R_{soil} and R_{h} with an assumption that the LI-8100 and FD chambers have no artifacts with respect to each other (Nickerson et al., 2013; Risk et al., 2011). Negative values (4.9% of total measurements) were excluded.

2.2.2. Measurements of R_{stem}

We measured CO_2 flux from the main stem surface (R_{stem}) for nine even-sized canopy dominant trees (three trees in each of the three ambient plots at EucFACE) using CO_2 flux measurement systems (LI-8100, Licor Environmental, Lincoln, NE, USA) coupled to a respiration chamber of 10 cm diameter (LI-8100-102) on PVC collars permanently attached to stems at 0.75 m height (Noh et al., 2021) (Figure S1 in Supporting Information S1). R_{stem} was measured during daytime hours (between 08:00 and 17:00) and 12 campaigns were conducted between January 2018 and February 2019 to achieve a wide temperature range across an entire year. R_{stem} was measured six times per tree within each campaign over 3 days to establish tree-specific relationships between R_{stem} and temperature. R_{stem} was calculated for each plot as the mean of the three trees and upscaled to the stand level on a per m^2 ground area basis by using the mean ratio of stem axial surface area per unit of soil surface area ($0.572 \text{ m}^2 \text{ m}^{-2}$) from terrestrial LiDAR (Jiang et al., 2020; Noh et al., 2021). The averaged scaling factor was applied to all three plots. R_{stem} was also measured continuously during day- and night-time using three forced diffusion (FD) chambers (Eosense eosFD, Dartmouth, Nova Scotia, Canada) by attaching them to the main stem at 1 m height (Figure S1 in Supporting Information S1). Data were collected every 30 min for the duration of the study period. We collected 93%, 70%, and 99% of the study period and non-gapfilled data were used to calculate apparent Q_{10} , a temperature sensitivity metric derived from spatial and temporal changes in temperature (Section 3). Flux data were removed when malfunction events were flagged by the eosFD software.

2.2.3. Eddy Covariance Based Estimates of R_{eco}

Net ecosystem exchange (NEE) was measured at the Cumberland Plain flux tower with a CSAT sonic anemometer (Campbell Scientific, Inc., Logan UT), LI-7500A infrared gas analyzer (Licor, Inc., Lincoln, NE), and profiler system integrated into PyFluxPro pipeline and processed according to TERN-OzFlux protocols (Isaac et al., 2017). Briefly, raw (10 Hz) data were cleaned and filtered ($u^* > 0.2 \text{ m s}^{-1}$) with EddyPro (Burba et al., 2013) within the SmartFlux-2 processing unit (Licor, Inc., Lincoln NE) to provide half-hourly fluxes of NEE (Griebel et al., 2020). Quality-controlled NEE was gapfilled using incoming short-wave radiation (29 m height; CNR4 radiometer, Kipp&Zonen, Delft, the Netherlands), vapor pressure deficit, air temperature (29 m height; HMP45, Vaisala, Finland), soil temperature (5 cm depth; Campbell T-107 thermocouple Logan, UT, USA), and soil water content (5 cm depth; CS616, Campbell Scientific, Logan UT) before partitioning NEE into $R_{\text{eco,eddy}}$ and GPP components utilizing the SOLO neural network from PyFluxPro (Isaac et al., 2017). SOLO was trained on air temperature, soil temperature, and soil moisture; however, non-gapfilled data were used for Q_{10} estimation (Section 2.2.5).

2.2.4. Meteorological Drivers for R_{eco} and Its Respiration Components

At the EucFACE site, air temperature (T_{air}), stem surface temperature (T_{stem}), leaf temperature (T_{leaf}), and soil temperature (T_{soil}) were measured at half-hourly resolution. T_{air} was measured at 2 m height at six locations using HMP155 sensors (Vaisala, Vantaa, Finland). T_{stem} was measured with copper-constantan type-T thermocouples inserted to a 3 cm depth into the three stems and 5 cm below the stem collars. T_{leaf} was measured half-hourly on canopy surfaces of 24 trees (one sensor per tree) using infrared thermometers (SI-121-L10, Apogee Instruments, Inc., USA). T_{soil} was measured at 5 cm soil depth within 1 m of the auto-chambers. The soil volumetric water content (θ) was measured half-hourly at six different locations with two sets of probes installed at 5 and 35 cm soil depths (ThetaProbes ML2x, Delta-T Devices Ltd, Cambridge, UK).

2.2.5. CABLE-POP Modeled Respiration Components

The land surface model CABLE-POP (Haverd et al., 2018) simulates exchanges of carbon, water, and energy between the land surface and the atmosphere. The two main components are a biogeophysical core module (Wang & Leuning, 1998) and a biogeochemistry module (Wang et al., 2010), which simulates carbon, nitrogen, and phosphorous cycling at a daily time step. The model simulates R_{h} from soil carbon and litter pools and R_{a} from growth and maintenance respiration from leaves, stems, and fine roots separately, as described in detail below

(Haverd et al., 2018; Wang et al., 2010). In the new version used here (r7523), R_h was calculated following the DAMM model (Davidson et al., 2012; Sihi et al., 2018). Modeled R_{eco} was defined as sum of R_h and R_a .

CABLE-POP distinguishes three soil carbon pools (microbial, slow, passive) and three litter pools (metabolic, structural, coarse woody debris) which differ with respect to their turnover times. Daily heterotrophic respiration of soil carbon ($R_{h,soil}$) is calculated as:

$$R_{h,soil} = \sum_{p=1}^{n_{pool}} k_{soil,p} \cdot C_{soil,p} \quad (1)$$

where $k_{soil,p}$ (day^{-1}) is the turnover rate for soil pool p and $C_{soil,p}$ (kg C m^{-2}) is the carbon content of pool p . k_{soil} for each soil pool is given by:

$$k_{soil,mic} = x_{soil} \cdot k_{base,mic} \cdot (1.0 - 0.75 \cdot (f_{silt} + f_{clay})) \quad (2)$$

$$k_{soil,slow} = x_{soil} \cdot k_{base,slow} \quad (3)$$

$$k_{soil,pass} = x_{soil} \cdot k_{base,pass} \quad (4)$$

where x_{soil} is a rate modifier, k_{base} is a base turnover rate (day^{-1}) for each soil pool (see Table S2 in Supporting Information S1), f_{silt} and f_{clay} are soil fractions of silt and clay, respectively. The rate modifier x_{soil} was calculated according to the DAMM model (Sihi et al., 2018):

$$x_{soil} = 10^\alpha \cdot f(T) \cdot f(M) \quad (5)$$

where α is a pre-exponent factor representing base respiration and $f(T)$ and $f(M)$ are temperature and moisture response functions, respectively:

$$f(T) = \frac{\exp\left(-\frac{E_a}{R_{gas} \cdot T_{soil}}\right)}{\exp\left(-\frac{E_a}{R_{gas} \cdot T_{ref}}\right)} \quad (6)$$

$$f(M) = \frac{[Enz]}{K_{enz} + [Enz]} \cdot \frac{[O_2]}{K_{O_2} + [O_2]} \quad (7)$$

where E_a is the activation energy ($62,000 \text{ J mol}^{-1}$) (Table S2 in Supporting Information S1), R_{gas} is the universal gas constant ($8.314 \text{ J mol}^{-1} \text{ K}^{-1}$), T_{soil} is the root fraction-weighted average soil temperature (K), and T_{ref} is the reference temperature (283 K). $[Enz]$ is the modeled concentration of active enzymes (mg C cm^{-3}) dependent on the thickness of soil water films (Sihi et al., 2018):

$$[Enz] = \text{EnzPool} \times \text{DI} \times \theta^3 \quad (8)$$

where DI is the diffusivity of enzymes in liquid and θ is the volumetric soil water content (Table S1 in Supporting Information S1). EnzPool (the enzyme pool in the soil solution, mg C cm^{-3} ; Table S2 in Supporting Information S1) and α were constrained by calibrating CABLE-POP against quality filtered observations of evapotranspiration, and net ecosystem production (from eddy covariance data) and soil respiration (from chamber measurements) at the site from 2014 to 2017 using the PEST optimization package (model-independent Parameter Estimation and Uncertainty Analysis, <http://www.pesthomepage.org/>) (Renchon, 2019). For the optimization and all subsequent simulations, the model was forced with meteorological data measured at the site. $[O_2]$ is the oxygen concentration (mol mol^{-1}), and K_{enz} (mg C cm^{-3}) and K_{O_2} (mol mol^{-1}) are the Michaelis-Menten constants for active enzymes and O_2 , respectively. $[O_2]$ in the soil is calculated as:

$$[O_2] = D_{va} \cdot f_{air}^{4/3} \quad (9)$$

where D_{va} is the diffusion coefficient for O_2 in air and f_{air} is the air-filled porosity of the soil. We accounted for the temperature dependency of D_{va} following Haverd and Cuntz (2010). The power function represents tortuosity in diffusion path length for O_2 in soil. For more information, see Davidson et al. (2012) and Sihi et al. (2018).

Equivalent formulations have been implemented for respiration of the three litter pools (metabolic, structural, coarse woody debris) whose turnover rates are calculated in the same way as the slow and passive soil pools (Equations 3 and 4) but with different base turnover rates (k_{base} , see Table S2 in Supporting Information S1). Calculation of the DAMM rate modifier for litter was assumed identical to the one for soil ($x_{litter} = x_{soil}$; Equations 6–9). Simulated R_h is summed across soil and litter components.

R_a is the sum of maintenance respiration (R_{main}) and growth respiration (R_{growth}). CABLE-POP simulates maintenance respiration from leaves, stem components, and fine roots separately. Leaf maintenance respiration ($R_{main,leaf}$; $\mu\text{mol m}^{-2} \text{s}^{-1}$) depends on the maximum carboxylation capacity at 25°C ($V_{cmax,25}$; $\mu\text{mol m}^{-2} \text{s}^{-1}$) and acclimates to temperature (Atkin et al., 2015). For evergreen broadleaf trees, the following relationship is used:

$$R_{main,leaf} = 1.2818 + 0.0116 * V_{cmax,25} - 0.0334 * TWQ * f_{Rd} \quad (10)$$

where TWQ is the air temperature of the warmest quarter (°C) and $V_{cmax,25}$ is modeled as a function of leaf N content following Walker et al. (2014). f_{Rd} is calculated as:

$$f_{Rd} = \left(3.09 - 0.043 \left(\frac{T_{leaf} + 25.0}{2} \right) \right)^{\left(\frac{T_{leaf} - 25.0}{10} \right)} * f_{wsoil} * \Pi * f_{PAR} \quad (11)$$

where T_{leaf} is leaf temperature (°C), f_{wsoil} is a water stress scalar (Haverd et al., 2013), Π is a factor describing the scaling from leaf-to-canopy level (Wang & Leuning, 1998), and f_{PAR} is a function accounting for light inhibition of $R_{main,leaf}$ (Brooks & Farquhar, 1985). The temperature response for $R_{main,leaf}$ (first term in Equation 11) was calculated following Atkin et al. (2015).

Note that $R_{main,leaf}$ is the only respiration component that is calculated at the half-hourly time scale in the model, while all other components (i.e., stem and fine roots) are calculated at daily time scales.

Maintenance respiration of stem (including coarse roots) and fine roots is given by:

$$R_{main,x} = c_{r,x} \cdot r_{base,x} \cdot \exp \left(308.56 \cdot \left(\frac{1.0}{56.0} - \frac{1.0}{T + 46.02 - 273.15} \right) \right) \quad (12)$$

where $c_{r,x}$ is a component-specific respiration coefficient depending on temperature and tissue nitrogen content (gN m^{-2}), $r_{base,x}$ is the base maintenance respiration rate. The subscript x represents stems and fine roots, respectively. The temperature response is modeled as a hyperbolic response function where T (°C) represents air temperature for $R_{main,stem}$, and soil temperature for $R_{main,fineroot}$. See Table S2 in Supporting Information S1 for a list of parameter or variable values.

Growth respiration is calculated at the whole plant level:

$$R_{growth} = (1 - G_{eff}) \cdot (GPP - R_{main}) \quad (13)$$

where G_{eff} is the efficiency of growth respiration which is estimated from the ratio of leaf phosphorus content to leaf nitrogen content (PN_{leaf}):

$$G_{eff} = 0.65 + 0.2 \frac{PN_{leaf}}{PN_{leaf+1/15}} \quad (14)$$

For this study, R_{growth} was divided into leaf, stem, and fine root components by assuming that the fraction of R_{growth} attributed to a specific plant component x equals the fraction of NPP allocated to the respective component ($f_{Alloc,x}$):

$$R_{\text{growth},x} = f_{\text{Alloc},x} \cdot R_{\text{growth}} \quad (15)$$

3. Data Analyses

While we use Arrhenius and hyperbolic temperature functions in the models, we use the more simplistic apparent Q_{10} metric to compare measured respiration rates to reported literature values and across observed and simulated R components. The term “apparent” is used to indicate that these are observed or model-output temperature responses that may also be affected by other confounding environmental factors, such as soil moisture, vapor pressure deficit or substrate supply, and do not necessarily reflect intrinsic temperature sensitivities of the enzymes when unlimited by other environmental constraints (Davidson & Janssens, 2006). The exponential function was applied only to non-gapfilled observations:

$$R_{\text{component}} = a \cdot e^{bT} \quad (16)$$

where $R_{\text{component}}$ is the CO_2 flux per unit surface area ($\text{g C m}^{-2} \text{d}^{-1}$) from respiration components, T is either leaf, stem, root, or soil temperature ($^{\circ}\text{C}$), a and b are fitting parameters. We calculated the apparent temperature sensitivity of respiration rates by using non-gapfilled data in the following exponential function:

$$Q_{10} = e^{10 \times b} \quad (17)$$

where b is the fitting parameter from Equation 16. We also calculated normalized R_{10} at measurement temperature of 10°C as a basal respiration rate of each component. R at any measured temperature T is predicted using the following equation:

$$R = R_{10} \cdot Q_{10}^{(T-10)/10} \quad (18)$$

where R_{10} and Q_{10} are basal respiration and apparent temperature sensitivity for each component.

Direct, canopy-scale respiration (R_{canopy}) measurements were not possible so they were calculated from leaf respiration (R_{leaf}) and scaled by temperature and leaf area (Ouimette et al., 2018). R_{leaf} was measured over a leaf temperature (T) gradient for the study years and used to fit the following equation:

$$R_{\text{leaf}} = R_{25} \cdot k_T^{(T-25)/25} \quad (19)$$

where R_{25} was R at 25°C , the value of which was taken as $1.3 \mu\text{mol m}^{-2} \text{s}^{-1}$ for the night time, and $0.9 \mu\text{mol m}^{-2} \text{s}^{-1}$ during the daytime, and k_T was a regression coefficient of 0.078 (Yang et al., 2020). Daily R_{leaf} was upscaled to R_{canopy} at the stand level with hourly average air temperature used as T and daily values of overstory leaf area index ($0.20\text{--}1.42 \text{ m}^2 \text{ m}^{-2}$, Figure S2 in Supporting Information S1) for the study period of 2018–2019 (Yang et al., 2020). Estimates of apparent Q_{10} and R_{10} of R_{canopy} were recalculated using Equation 17, where b was k_T , and Equation 18, respectively.

To estimate annual R rates, we gapfilled using hourly T from stem, canopy, air, and soil at 5 cm-depth throughout the entire year. Microbial respiration (R_h) was gapfilled with the DAMM model (Arrhenius temperature sensitivity modified by substrate supply). The remaining root, stem, and canopy R components were gapfilled with observed apparent Q_{10} functions. Measured R_{eco} at stand level ($R_{\text{eco.sum}}$) was determined as the sum of its gapfilled components (R_h , R_{root} , and R_{stem}) and R_{canopy} .

4. Results

4.1. Seasonal Variations in Temperature and Soil Moisture

The seasonal patterns of air, leaf, stem, and soil temperature were characterized by a warm spring/summer/autumn period from October to March and a cool period from April to September (Figures 1a and 1b). During the study period, daily mean temperature varied between 5.2 and 31.2°C for air, 6.2 and 31.8°C for leaf, 8.1 and 31.2°C for stem in 15 July 2018 and 7 January 2018, respectively, and between 8.8°C (16 July 2018) and 30.6°C

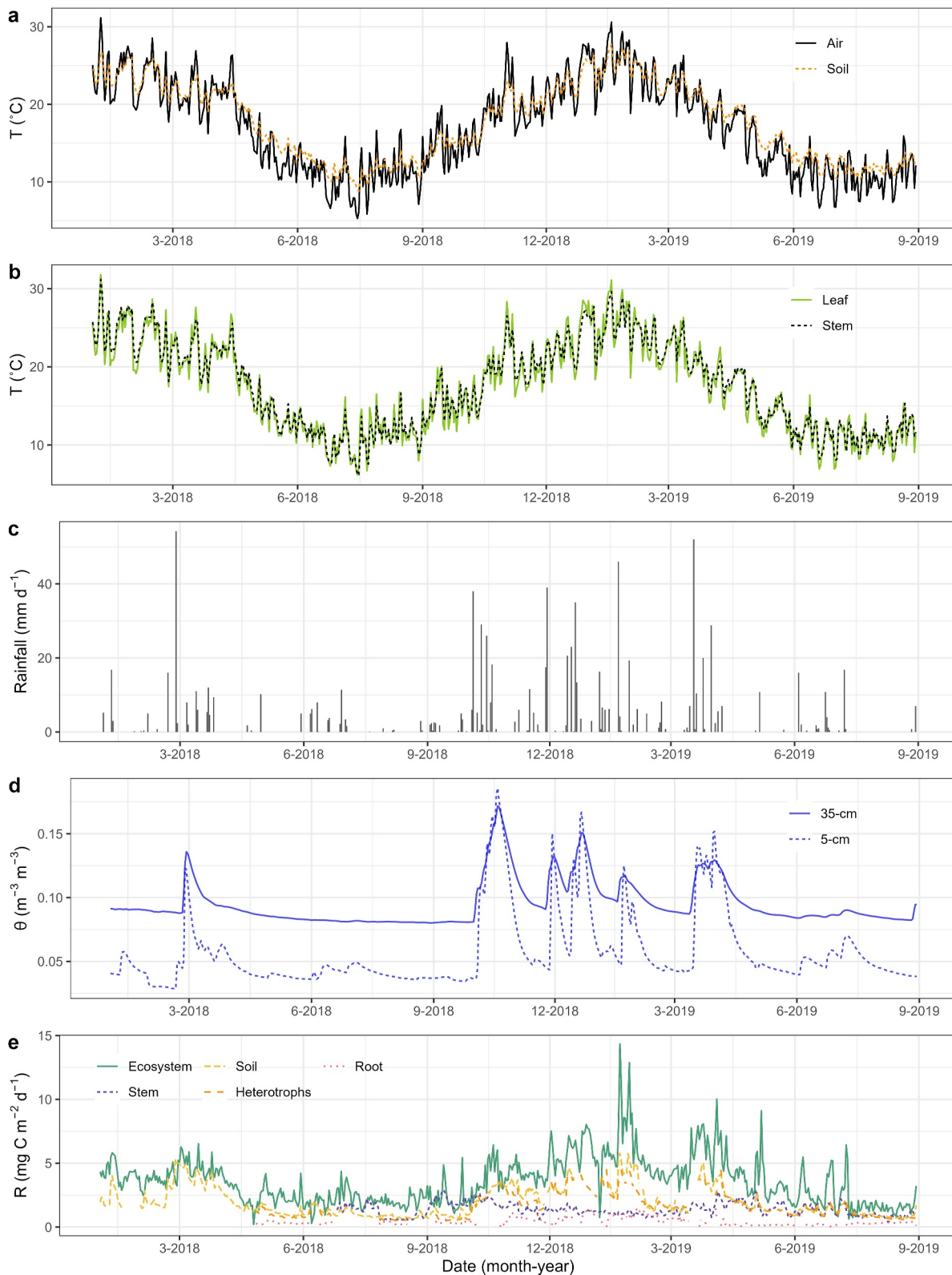


Figure 1. Seasonal variations in daily values of (a) temperature (T) of air and soil, (b) T of leaf and stem surface, (c) rainfall, (d) soil volumetric water content (θ), and (e) daily mean respiration rate (R). Ecosystem respiration is estimated by eddy covariance method and gapfilled with a neural network, soil respiration is measured by auto-chambers (Li-8100A), heterotrophic respiration and stem respiration are measured by Forced diffusion auto-chambers (eosFD), and root respiration is estimated by the difference between total soil respiration and heterotrophic respiration.

Table 1

Measured and Simulated Basal Respiration Per Unit Ground Area (R_{10} , $\text{mg C m}^{-2} \text{d}^{-1}$), Apparent Temperature Sensitivity (Q_{10}) of Non-Gapfilled Respiratory Components, Annual Respiration Rate Per Unit Ground Area (R , $\text{g C m}^{-2} \text{yr}^{-1}$), and the Percent Contribution of (Gapfilled) Respiratory Components to Ecosystem Respiration Estimated From September 2018 to August 2019

R component	Field measurements					CABLE-POP				
	R_{10}	Q_{10}	R^2	Annual R	% cont.	R_{10}	Q_{10}	R^2	Annual R	% cont.
R_{canopy}^a	0.10	4.33	0.951	168	13.0	0.56	1.41	0.584	276	21.3
R_{stem}	0.47	1.86	0.145	291	22.5	0.60	1.37	0.721	284	21.9
R_{soil}	0.93	2.38	0.562	811	64.5	1.09	2.00	0.901	737	56.8
R_h	0.74	2.45	0.584	636	49.1	0.75	2.34	0.898	595	45.9
R_{root}^b	0.15	2.65	0.344	200	15.4	0.36	1.09	0.065	142	11.0
$R_{\text{eco.sum}}$	1.75	2.22	0.833	1,295	100	2.46	1.57	0.850	1,297	100
$R_{\text{eco.eddy}}$	1.93	2.15	0.552	1,439	–					

^a R_{canopy} was scaled from Q_{10} (2.18) and R_{10} (0.37) of R_{leaf} and continuously measured leaf area (Yang et al., 2020); see Figure S2 in Supporting Information S1. ^b R_{root} was determined as the difference of $R_{\text{soil}} - R_h$.

(18 January 2019) for soil. The volumetric soil moisture fluctuated with rainfall (Figures 1c and 1d) and varied between 2.9% and 18.6% at 5 cm soil depth and 8.0% and 17.2% at 35 cm soil depth.

4.2. Seasonal Variations in R_{eco} and Its Components

Most R_{eco} components showed a similar seasonal trend to that of temperature throughout the year with the lowest respiration rates during the cold season and the highest rates during the warm season (Figure 1e). The highest daily mean $R_{\text{eco.eddy}}$ was $14.3 \text{ g C m}^{-2} \text{d}^{-1}$ (22 January 2019) with peaks in mid-summer coinciding with the highest daily mean R_{soil} of $5.8 \text{ g C m}^{-2} \text{d}^{-1}$ (22 January 2019) and R_h of $4.6 \text{ g C m}^{-2} \text{d}^{-1}$ on 23 January 2019. The second phase of peaks in $R_{\text{eco.eddy}}$ was observed in autumn (March–April), coinciding with the highest daily mean R_{root} of $1.5 \text{ g C m}^{-2} \text{d}^{-1}$ (3 April 2019) and highest daily mean R_{stem} of $2.8 \text{ g C m}^{-2} \text{d}^{-1}$ (5 April 2019) although R_{root} above $1.0 \text{ g C m}^{-2} \text{d}^{-1}$ and R_{stem} above $2.0 \text{ g C m}^{-2} \text{d}^{-1}$ were mainly observed in summer.

4.3. Responses of Respiration Components to Temperature

R_{eco} and its components increased with increasing temperature and the apparent Q_{10} of $R_{\text{eco.eddy}}$ from eddy flux observation was 2.15, comparable to that of the sum of the components (2.22) (Table 1, Figure S3 in Supporting Information S1). Apparent Q_{10} values were 2.38 for R_{soil} , 2.45 for R_h , 1.86 for R_{stem} , and 4.33 for R_{canopy} (Table 1; Figure S2 in Supporting Information S1). Apparent Q_{10} values inferred from CABLE-POP outputs for R_{canopy} , R_{stem} , and R_{root} were all considerably lower than those based on non-gapfilled observations, whereas apparent Q_{10} of R_h of 2.34 inferred from CABLE-POP was comparable to the field-measured apparent Q_{10} of 2.45.

4.4. The Measured Contributions of Respiration Components to R_{eco}

$R_{\text{eco.sum}}$ and its components all generally followed the seasonal pattern of temperature with spikes following wet-up events (Figures 1 and 2a). The mean contribution of respiration components to annual $R_{\text{eco.sum}}$ was 64.5% for soil, 22.5% for stem, and 13.0% for canopy leaves (Table 1). The mean contribution of R_h to total R_{soil} was 76% and that of R_{root} was 24%. The contribution of respiration components to the $R_{\text{eco.sum}}$ differed between the seasons. R_{soil} ($R_h + R_{\text{root}}$) contributed from 42% to 77% of $R_{\text{eco.sum}}$ across the study period, while R_{stem} contributed up to 42% of $R_{\text{eco.sum}}$ during the colder months of August and September and 14% of $R_{\text{eco.sum}}$ in March (Figure 2b). R_{canopy} showed a high seasonality in its contribution to $R_{\text{eco.sum}}$ contributing 4%–37% of $R_{\text{eco.sum}}$ across the study period. R_{root} also showed strong seasonality but smaller magnitude contributing 4%–10% of $R_{\text{eco.sum}}$.

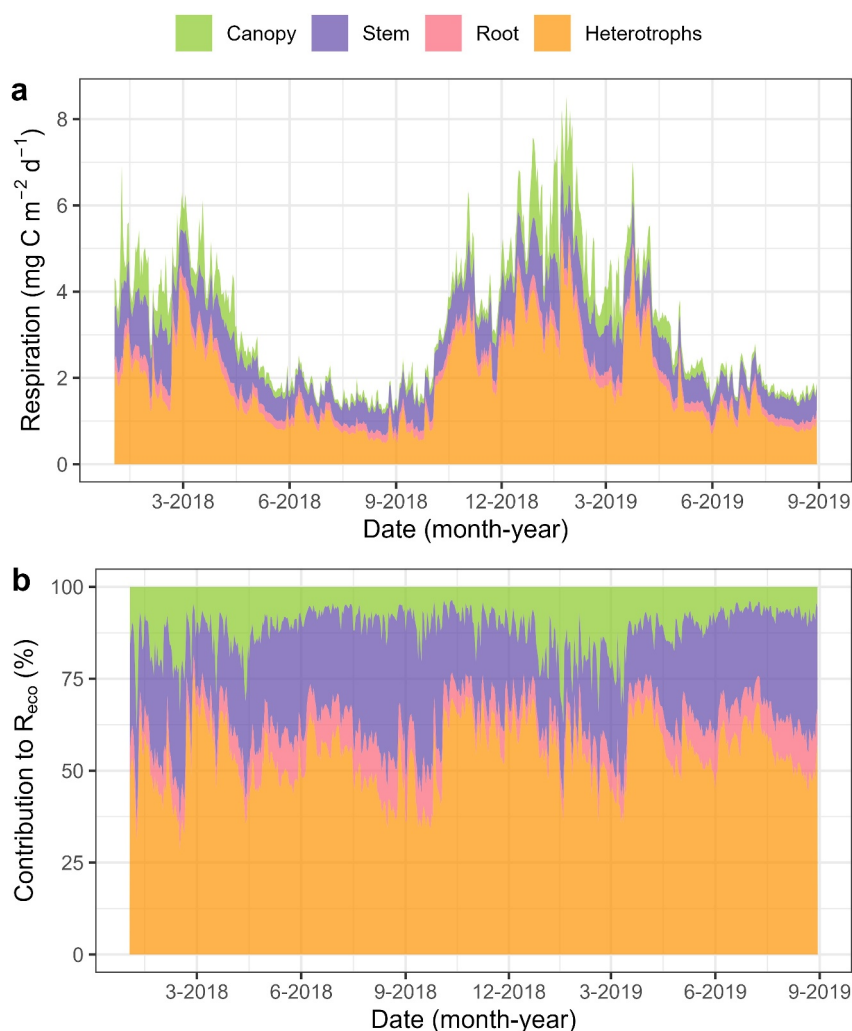


Figure 2. (a) Estimates of measured seasonal respiratory components of R_{eco} and (b) their contributions to R_{eco} . Estimates were calculated from empirical temperature relationships (the coefficients of R_{10} and Q_{10} for each component shown in Table 1). The percentage values in (b) indicate the average daily contribution for each component during the measurement period. Note that R_{root} was estimated as the difference between R_{soil} and R_h .

4.5. Comparisons of Measurements to Modeled Respiration Rates

Chamber measurements and temperature response functions were used to scale up from soil, stem, and leaf to the stand level ($R_{eco, sum}$) for comparison with $R_{eco, eddy}$ and $R_{eco, CABLE}$ (Table 1). On an annual basis, outputs of CABLE-POP model were lower than the chamber-based respiration rates, by 2.4% for stem, 6.5% for heterotrophs, and 29.0% for root, whereas the CABLE-POP output for R_{canopy} was 64.2% higher than that estimated as a function of temperature, leaf Q_{10} and leaf area (Table 1). The CABLE-POP model did not capture the range of observations for the R_a components (Figures 3a–3c and 3e) but modeled values gave reasonable fits to observed R_h ($R^2 = 0.673$, $RMSE = 0.606$) and R_{soil} ($R^2 = 0.656$, $RMSE = 0.749$) (Figures 3c and 3d). The DAMM module fit observed R_h better than other decomposition algorithms including Lloyd and Taylor and the default CASA approach when slope biases are taken into account (Figure S4 in Supporting Information S1).

The annual $R_{eco, sum}$ calculated as the sum of the components ($1,295 \text{ g C m}^{-2} \text{ yr}^{-1}$) was similar to that predicted by the CABLE-POP model ($1,297 \text{ g C m}^{-2} \text{ yr}^{-1}$), and these estimates were both about 10% lower than the $R_{eco, eddy}$ calculated based on eddy covariance measurements ($1,439 \text{ g C m}^{-2} \text{ yr}^{-1}$) (Table 1). There

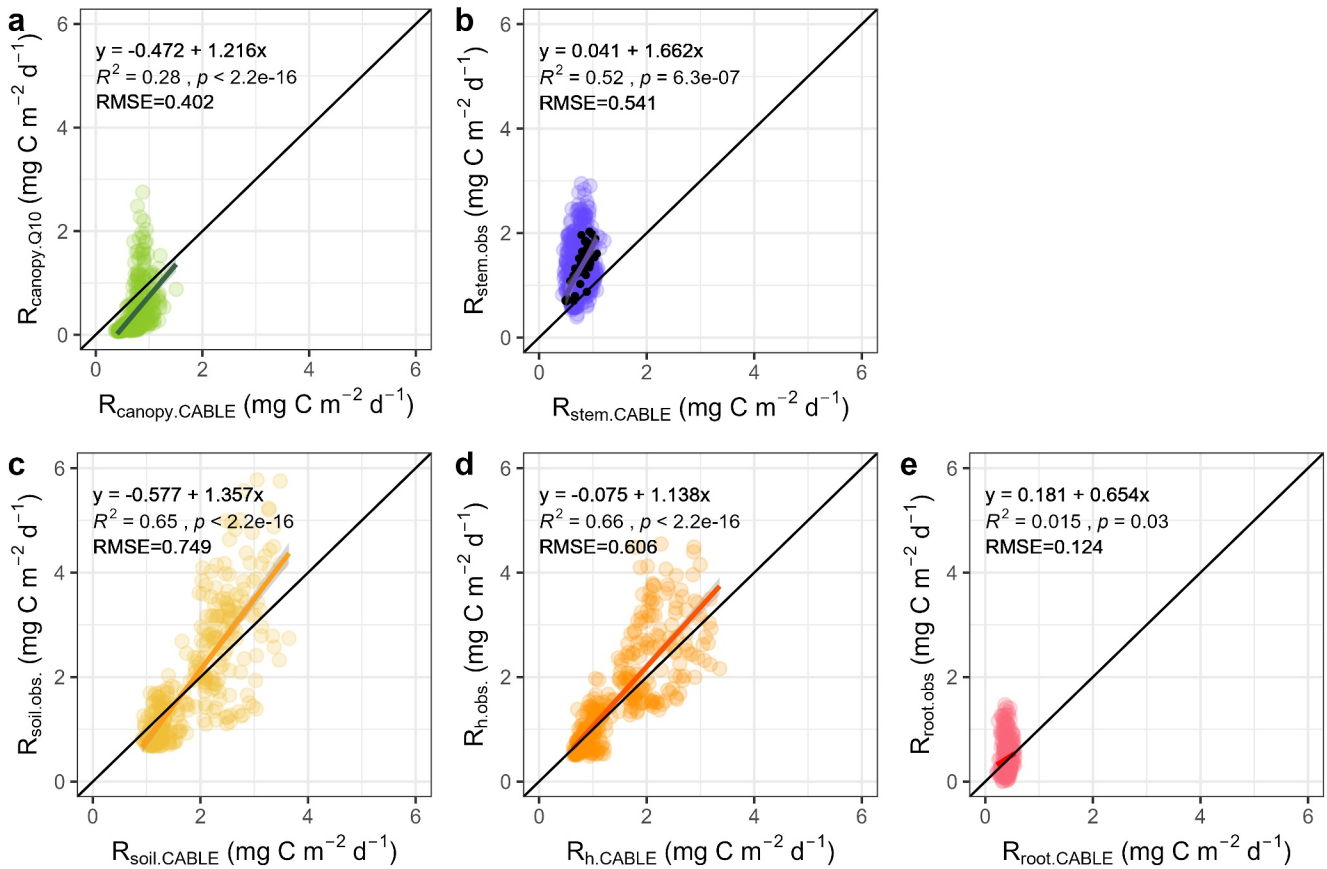


Figure 3. Comparison of CABLE-POP model outputs with non-gapfilled measurements of the respiration components. (a) Canopy respiration ($R_{\text{canopy.Q10}}$; the plotted data were reproduced from an empirical model using Q_{10} of canopy leaves and canopy temperature as inputs), (b) stem respiration ($R_{\text{stem.obs}}$; continuously measured by eosFD, black circles, and R_{stem} monthly measured by Li-8100, purple circles), (c) soil respiration (R_{soil}), (d) heterotrophic soil respiration (R_{h}), and (e) root respiration (R_{root}). The black and colored lines indicate 1:1 line and linearly fitted regression line, respectively. The R^2 and root mean square error (RMSE) are shown in the panels.

were significant correlations among observed and simulated respiration rates (all $p < 0.001$, $R^2 > 0.55$, $\text{RMSE} < 0.857 \text{ mg C m}^{-2} \text{ d}^{-1}$, Figure 4). The agreement between $R_{\text{eco.eddy}}$ and $R_{\text{eco.sum}}$ was very good with slope of 0.95 (Figure 4a), whereas relationships with modeled R_{eco} demonstrated that CABLE-POP overestimated low values and underestimated high values compared to observations (Figures 4b and 4c).

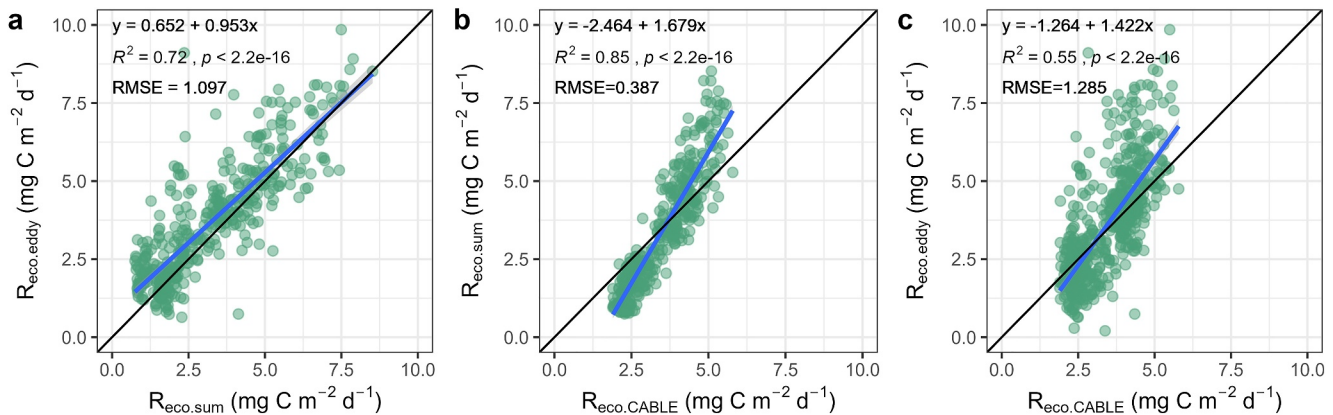


Figure 4. Relationships for daily measured and modeled R_{eco} in a mature eucalypt forest. $R_{\text{eco.sum}}$ was calculated as the sum of heterotrophic, root, stem, and canopy respiration measurements, $R_{\text{eco.eddy}}$ was derived from measured and gapfilled NEE at the AU-Cum flux tower, and $R_{\text{eco.CABLE}}$ was output from CABLE-POP. (a) $R_{\text{eco.eddy}}$ versus $R_{\text{eco.sum}}$, (b) $R_{\text{eco.sum}}$ versus $R_{\text{eco.CABLE}}$, (c) $R_{\text{eco.eddy}}$ versus $R_{\text{eco.CABLE}}$. The black and blue lines indicate 1:1 line and regression line, respectively. The equation of the regression, R^2 and root mean square error (RMSE) are shown in the panels.

5. Discussion

At our warm-temperate eucalypt-dominated site, net C uptake occurs in cool months and net loss occurs during summer when R_{eco} dominates NEE (Renchon et al., 2018) providing motivation for improved understanding of the contributions of component fluxes. The present investigation found that concurrent scaled chamber measurements agreed with flux tower observations to within 10% and that soil microbial decomposition (R_h) is by far the largest respiratory pathway. We implemented the Dual Arrhenius Michaelis-Menten substrate availability function for R_h into the CABLE-POP land-surface model, and the simulations of the R_h component matched the observations better than the autotrophic components of roots, stems, or canopy. Apparent Q_{10} values estimated from observations were generally higher than those that emerged from CABLE-POP output, except for R_h , indicating a need for further improvements in observing, scaling, and modeling R_a . Scaling direct observations of component fluxes and their drivers to the ecosystem level allowed testing and improvement of a land-surface model which in turn helped identify and reconcile discrepancies between bottom-up and top-down methods.

5.1. Quantifying and Scaling Components of R_{eco}

Our field measurements identified a large contribution (49%) of R_h to $R_{\text{eco.sum}}$ in this mature forest which was close to 46% from CABLE-POP model outputs (Table 1). The contribution of R_{soil} to $R_{\text{eco.sum}}$ (64%) across the seasons in this study site is within the range of 30%–80% described for forest ecosystems (Davidson et al., 2006). We also observed variations in the contributions of R_{soil} to $R_{\text{eco.sum}}$ which reached a minimum of about 33% in the early spring and increased up to 70% in autumn when fine root biomass showed peak values (Piñeiro et al., 2020) and substrate for heterotrophic respiration in litter layer increased (Brændholt et al., 2018; Davidson et al., 2006). Our estimated contribution of R_{stem} to annual $R_{\text{eco.sum}}$ was approximately 22% which was higher than 8%–18% observed in 67-year-old pine and oak forests (Khomik et al., 2010; Rodríguez-Calcerrada et al., 2014). We also observed variations in the contributions of R_{stem} to $R_{\text{eco.sum}}$, which reached a minimum of about 14% in March and increased up to 42% in September, which is comparable to 6%–23% observed in a 115-year-old beech forest (Guidolotti et al., 2013). The contribution of R_h to R_{soil} was approximately 78% which is high compared to $63\% \pm 16\%$ based on global soil respiration database in 2007–2014 (Bond-Lamberty et al., 2018). Our R_h estimate could be overestimated by artifacts of root exclusion method due to increased soil water content in trenched plots (Savage et al., 2018). The estimated contribution of R_{root} was higher during cooler months, whereas that of R_{canopy} was higher during warmer months (Figure 2b), suggesting seasonal variations in carbon allocation to above-ground and belowground biomass that could be incorporated into future model versions (Merganičová et al., 2019; Renchon et al., 2024).

5.2. Temperature Sensitivities of R_{eco} and Its Components

Temperature sensitivity of R_{eco} is a crucial parameter for predicting the fate of CO_2 under global warming, and Earth system models are moving away from using a constant Q_{10} value of 2 to generate carbon dynamics in terrestrial ecosystems (Davidson et al., 2006; Johnston et al., 2021; Mahecha et al., 2010). Recently, Niu et al. (2021) reported that the average apparent Q_{10} of $R_{\text{eco.eddy}}$ derived from multiyear observations was 1.94 across 74 FLUXNET sites. Our estimate of 2.15 for the apparent Q_{10} of $R_{\text{eco.eddy}}$ is close to the average reported by Niu et al. (2021). The Q_{10} of R_{soil} (2.38) was comparable to that of $R_{\text{eco.eddy}}$ which makes sense because R_{soil} is the main component of R_{eco} in our site (Barba et al., 2018; Renchon et al., 2021; Figure 2). Despite widespread evidence for global coherence of Q_{10} for R_{eco} (Mahecha et al., 2010), recent studies suggest the need to consider a thermal optimum (Chen et al., 2023) or a sigmoidal function with lower temperature response at high temperatures (Zhang et al., 2021). These approaches recognize fundamental biochemical properties of enzymes (Fanin et al., 2022; Liang et al., 2018) and demonstrate an increasingly mechanistic understanding of temperature sensitivity at the ecosystem level.

Our observed value for apparent Q_{10} of R_{canopy} was unrealistically high (4.33) as R_{leaf} was upscaled to stand level with overstory leaf area varying seasonally (Table 1, Figure S2 in Supporting Information S1). This indicates that apparent Q_{10} of R_{canopy} upscaled based on empirical leaf-level Q_{10} (2.18 for unit leaf area; Yang et al., 2020) includes seasonal changes in leaf surface area or biomass (Figure S2d in Supporting Information S1). It may be an overestimate also considering that upper-canopy leaves were measured at our site and have significantly higher temperature sensitivity than lower in the canopy, due to their higher nitrogen concentrations (Turnbull et al., 2003). On the other hand, the inferred Q_{10} (1.41) of R_{canopy} from CABLE-POP outputs is more in line with

theoretical expectations given the mean annual temperature at our site. This value could emerge because the model encapsulates appropriate physiological functions including nitrogen, substrate supply, light inhibition, and thermal acclimation (Equation 10) (Haverd et al., 2018).

Chamber measurements of apparent Q_{10} for individual leaves (2.18; Yang et al., 2020), stems (1.86), and roots (1.69 for detached roots; Figure S5 in Supporting Information S1) were less sensitive to temperature changes than observed for non-gapfilled R_h (2.45) (Table 1). Respiratory metabolism in environments with wider fluctuations of air temperature can exhibit an increased acclimation capacity to temperature changes compared to the narrower fluctuations of soil temperature (Tjoelker et al., 2009). A review by Wang et al. (2006) found significant differences in mean Q_{10} among respiratory components of non-photosynthetic organs and soils of forest ecosystems showing the trend of soil (2.74) > root (2.40) > stem (1.91). A recent field study in subtropical forests reported that Q_{10} of respiratory components decreased along the vertical gradient of soil > stem > leaf (Chi et al., 2020).

For the component fluxes at our study site, the apparent Q_{10} of R_{stem} was lower than other components since it had a low seasonal amplitude (Noh et al., 2021), while the apparent Q_{10} of our inferred R_{root} (2.65) was higher than other components due to low rates at low temperature supporting the finding that roots can enhance the Q_{10} of total R_{soil} (Li et al., 2020). But as the R_{root} was estimated as the difference between R_{soil} and R_h , its magnitude and apparent Q_{10} could be affected by seasonal changes in fine root production and standing biomass observed at this site (Piñeiro et al., 2020) and by artifacts of the trenching method. Indeed, the apparent Q_{10} estimated in this way (2.65) was higher than from detached roots (1.69, Figure S5 in Supporting Information S1) because it includes the effects of seasonal variation in root growth, allocation of photosynthate to existing roots and mycorrhizae in addition to the temperature sensitivity per gram root and responses of root respiration to confounded changes in soil drying and wetting through time (Vargas & Allen, 2008). Thus, the apparent Q_{10} estimate for R_{root} reflects multiple processes that covary with temperature and does not represent the temperature sensitivity of the respiratory enzymes alone. The root Q_{10} inferred from CABLE-POP (1.09) was surprisingly low, potentially because allocation fractions to roots and other plant components in the model were relatively constant through the year (Table 1; Figure S5 in Supporting Information S1). Clearly, additional work is needed to reconcile observed and modeled estimates of root respiration and its temperature sensitivity.

The emergent Q_{10} value for R_h derived from the CABLE-POP output was remarkably similar to that based on root-exclusion soil respiration measurements suggesting that the incorporation of the semi-mechanistic DAMM model approach adequately predicts soil respiration dynamics. It should be noted that the R_h data were not used to parameterize CABLE-POP. However, the field-based estimates of apparent Q_{10} values for R_{canopy} , R_{stem} , R_{soil} , R_{root} , and $R_{\text{eco.sum}}$ were all higher than those estimated from CABLE-POP outputs. These differences suggest that apparent Q_{10} estimates simplify the responses of physiological processes to multiple interacting environmental conditions operating on variable temporal and spatial scales, particularly as regulated by substrate supply (Davidson et al., 2006). Alternative formulations for estimating temperature sensitivity from observations, such as the sigmoidal approach used for R_{eco} (Zhang et al., 2021), should be tested for component respiration. Temperature sensitivity and fluxes in CABLE-POP could be improved by specifying seasonal dynamics of leaf area and fine root biomass in relation to confounding drivers such as soil water content (Merganičová et al., 2019; Piñeiro et al., 2020; Renchon et al., 2024).

5.3. Data-Model Comparisons Demonstrate How To Reconcile Top-Down and Bottom-Up Estimates

Reconciling the discrepancy between eddy covariance and scaled chamber respiration estimates in forest ecosystems remains a difficult challenge due to spatial and temporal variability of each respiration component (Renchon et al., 2021). In our study, the annual $R_{\text{eco.sum}}$ of 1,297 g C m⁻² yr⁻¹ was about 10% lower than 1,439 g C m⁻² yr⁻¹ for $R_{\text{eco.eddy}}$. By contrast, a recent synthesis reported 13% larger average annual R_{eco} summed from components than estimated by eddy covariance in temperate forests, likely due to advective losses (Wang et al., 2017). Nevertheless, R_{eco} summed from components was reported to be slightly lower than estimated by eddy covariance in a 74-year-old boreal aspen forest (Griffis et al., 2004) and 4- to 67-year-old temperate white pine forests (Khomik et al., 2010). Our lower $R_{\text{eco.sum}}$ might be explained by the empirical R_{canopy} not accounting for understory vegetation. The annual R_{canopy} (168 g C m⁻² yr⁻¹) estimated by empirical Q_{10} function was also less than that estimated by CABLE-POP (276 g C m⁻² yr⁻¹) modeled only for overstory vegetation (Table 1) indicating a mismatch in measuring and scaling of overstory R_{leaf} rates (Figure S2c in Supporting Information S1). The CABLE-POP model accounted for acclimation response of R_{leaf} to temperature (Atkin et al., 2015),

but it applied the same thermal acclimation response to leaf, root, and stem respiration despite different proportions of nitrogen and phosphorus contents in these components (Haverd et al., 2018), and despite the fact that the acclimation response used here has not been tested for components other than leaves. Unlike most models, CABLE-POP did account for light inhibition which therefore cannot explain the discrepancies between the two estimates (e.g., Campioli et al., 2016). Additionally, upscaled R_{canopy} observations may have been underestimated if our leaf area measurements were too low, if the R_{leaf} measurements were not representative of the full temperature range, and/or if the Q_{10} function inadequately captured variations due to thermal acclimation (Ouimette et al., 2018; Tjoelker et al., 2009). More research on R_{leaf} and R_{root} throughout forest canopies and belowground including both overstory and understory plants is required to improve both field measurement and modeling estimates, particularly in regions of fluctuating water availability (Renchon et al., 2024). Nevertheless, the results demonstrate that simultaneous chamber measurements can help verify flux tower observations (Campioli et al., 2016; Ouimette et al., 2018).

We also found a modest underestimation by modeled R_{eco} ($1,297 \text{ g C m}^{-2} \text{ yr}^{-1}$) compared to $R_{\text{eco,eddy}}$ ($1,439 \text{ g C m}^{-2} \text{ yr}^{-1}$) partly due to the low simulated contribution of R_{root} (11.0%) compared to observations (15.4%). Modeling R_{root} is more difficult than other components due to complexity in spatial and temporal variability in root-traits and their measurements (McCormack et al., 2017). It should be remembered that modeled R_{root} included only fine roots (<2 mm) whereas the field observations of soil respiration included all roots; including coarse root respiration in the modeled R_{stem} contributes errors to both component fluxes. Other possible reasons for the underestimation of R_{root} include unrealistic representation of fractional carbon allocation to fine roots as well as fine root turnover rates. Indeed, fine roots at the site include a large component of understory species which vary seasonally in response to water availability (Píñeiro et al., 2020). These processes are treated as relatively constant over time and are thus likely over-simplified in the model. Thus, the role of R_{root} in ecosystem carbon cycling would be better understood if biosphere models and field observations both included specific R_{root} according to root size, structure and function, and seasonal dynamics of fine root biomass (Píñeiro et al., 2020; Warren et al., 2015).

We found an inconsistency between modeled and observed R_{stem} (Figure 3c) with potential uncertainties in upscaling R_{stem} when we assumed that the stem surface area-based respiration rate at a certain point is constant throughout the stem. However, since previous studies reported that R_{stem} was greater inside the crown or near roots than at our measurement height of 1-m (Araki et al., 2010; Tarvainen et al., 2014; Zhao et al., 2018), actual R_{stem} may be greater than our observed estimate. Further, modeling R_{stem} should include monitoring multiple driving factors such as sap flow, xylem and soil water potential, and nonstructural carbohydrates (Salomón et al., 2020). Additional analyses of the seasonal variation of processes that contribute to observed apparent temperature sensitivities will be useful to inform formulations of thermal acclimation of root and stem respiration in models, which is a key uncertainty in predicting global carbon dynamics (Atkin et al., 2008; Lombardozzi et al., 2015; Noh et al., 2020).

Although temperature was one of major factors driving temporal variability of the components of R_{eco} , phenology is the dominant driver of canopy and photosynthesis processes (Renchon et al., 2024), which, in turn, are the critical drivers of respiration (Ouimette et al., 2018). The temperature response of respiration covaries with this phenology of photosynthesis and leaf growth which is partly why the apparent Q_{10} values are generally higher than 2. Therefore, other environmental factors such as water availability affecting phenology for leaves and roots should be considered for interpreting data-model comparisons (Guidolotti et al., 2013; Li et al., 2022; Matteucci et al., 2015). Indeed, water availability was found to be the key driver of R_h in water limited regions, based on machine learning results from a global data product (Yao et al., 2021). At our site, Drake et al. (2018) showed that apparent Q_{10} of R_{soil} increased from ~ 1.6 at low θ up to ~ 3 at high θ , possibly indicating covariation of temperature with substrate supply at higher water content (Davidson & Janssens, 2006). The CABLE-POP model outputs of R_h matched the observations well, which may be because the new DAMM module incorporated the relevant biophysical factors of substrate availability, temperature, and effects of soil water content including oxygen limitations for decomposition of soil organic matter.

6. Conclusions

This research demonstrated that bottom-up respiration component measurements can be successfully scaled to eddy covariance-based and simulated ecosystem fluxes. Cross-validation of $R_{\text{eco,eddy}}$ estimates by summing

chamber-based component measurements indicated that agreement within 10% (this study; Ouimette et al., 2018) to 15% is possible (Yuan et al., 2018). By comparing component respiration rates among field measurements, flux-tower observations and model estimates, this study provided mechanistic insights that are relevant to model development. In particular, including substrate limitation to R_h using the DAMM model improved CABLE-POP relative to four other approaches to estimating microbial respiration. However, a mismatch between observations and simulations for canopy and root components could be explained by challenges of estimating their temperature sensitivity in the field. Further model-data integration and modeling improvements should consider dynamic carbon allocation to different components, including root growth, exudation, mycorrhizae (Vargas & Allen, 2008), and storage (Montane et al., 2017), and thermal acclimation responses for simulating seasonal variations in autotrophic respiration, in particular for stem, root and mycorrhizal respiration (Atkin et al., 2008; Hopkins et al., 2013).

Data Availability Statement

All figures were made in the statistical software R version 4.2.3 (R Core Team, 2020). Field measurements and observation data sets for CO₂ fluxes and their drivers are available with CC BY 4.0 access (Pendall & Noh, 2024). The CABLE-POP code (r7523) is available on a public data repository (https://trac.nci.org.au/trac/cable/browser#branches/Users/jk8585/gm_acclim_coord).

Acknowledgments

This research was supported by the Australian Research Council (DP170102766 and DP220102039) and TERN-OzFlux, an NCRIS enabled facility. We thank C. McNamara, V. Kumar and D. Metzen for their excellent support for experiments and data sets from EucFACE and Cumberland Plain TERN sites. Open access publishing facilitated by Western Sydney University, as part of the Wiley - Western Sydney University agreement via the Council of Australian University Librarians.

References

- Araki, M. G., Utsugi, H., Kajimoto, T., Han, Q., Kawasaki, T., & Chiba, Y. (2010). Estimation of whole-stem respiration, incorporating vertical and seasonal variations in stem CO₂ efflux rate, of *Chamaecyparis obtusa* trees. *Journal of Forest Research*, 15(2), 115–122. <https://doi.org/10.1007/s10310-009-0163-3>
- Aspinwall, M. J., Drake, J. E., Company, C., Vårhammar, A., Ghannoum, O., Tissue, D. T., et al. (2016). Convergent acclimation of leaf photosynthesis and respiration to prevailing ambient temperatures under current and warmer climates in *Eucalyptus tereticornis*. *New Phytologist*, 212(2), 354–367. <https://doi.org/10.1111/nph.14035>
- Atkin, O. K., Atkinson, L. J., Fisher, R. A., Campbell, C. D., Zaragoza-Castells, J., Pitchford, J. W., et al. (2008). Using temperature-dependent changes in leaf scaling relationships to quantitatively account for thermal acclimation of respiration in a coupled global climate-vegetation model. *Global Change Biology*, 14(11), 2709–2726. <https://doi.org/10.1111/j.1365-2486.2008.01664.x>
- Atkin, O. K., Bloomfield, K. J., Reich, P. B., Tjoelker, M. G., Asner, G. P., Bonal, D., et al. (2015). Global variability in leaf respiration in relation to climate, plant functional types and leaf traits. *New Phytologist*, 206(2), 614–636. <https://doi.org/10.1111/nph.13253>
- Aubinet, M., Vesala, T., & Papale, D. (2012). *Eddy covariance: A practical guide to measurement and data analysis*. Springer.
- Baldocchi, D. (2014). Measuring fluxes of trace gases and energy between ecosystems and the atmosphere—The state and future of the eddy covariance method. *Global Change Biology*, 20(12), 3600–3609. <https://doi.org/10.1111/gcb.12649>
- Barba, J., Cueva, A., Bahn, M., Barron-Gafford, G. A., Bond-Lamberty, B., Hanson, P. J., et al. (2018). Comparing ecosystem and soil respiration: Review and key challenges of tower-based and soil measurements. *Agricultural and Forest Meteorology*, 249, 434–443. <https://doi.org/10.1016/j.agrformet.2017.10.028>
- Bond-Lamberty, B., Bailey, V. L., Chen, M., Gough, C. M., & Vargas, R. (2018). Globally rising soil heterotrophic respiration over recent decades. *Nature*, 560(7716), 80–83. <https://doi.org/10.1038/s41586-018-0358-x>
- Brændholt, A., Ibrom, A., Larsen, L. S., & Pilegaard, K. (2018). Partitioning of ecosystem respiration in a beech forest. *Agricultural and Forest Meteorology*, 252, 88–98. <https://doi.org/10.1016/j.agrformet.2018.01.012>
- Brooks, A., & Farquhar, G. (1985). Effect of temperature on the CO₂/O₂ specificity of ribulose-1, 5-bisphosphate carboxylase/oxygenase and the rate of respiration in the light. *Planta*, 165(3), 397–406. <https://doi.org/10.1007/BF00392238>
- Burba, G., Madsen, R., & Feese, K. (2013). Eddy covariance method for CO₂ emission measurements in CCUS applications: Principles, instrumentation and software. *Energy Procedia*, 40, 329–336. <https://doi.org/10.1016/j.egypro.2013.08.038>
- Campoli, M., Malhi, Y., Vicca, S., Luyssaert, S., Papale, D., Peñuelas, J., et al. (2016). Evaluating the convergence between eddy-covariance and biometric methods for assessing carbon budgets of forests. *Nature Communications*, 7(1), 13717. <https://doi.org/10.1038/ncomms13717>
- Carbone, M. S., Richardson, A. D., Chen, M., Davidson, E. A., Hughes, H., Savage, K. E., & Hollinger, D. Y. (2016). Constrained partitioning of autotrophic and heterotrophic respiration reduces model uncertainties of forest ecosystem carbon fluxes but no stocks. *Journal of Geophysical Research: Biogeosciences*, 121(9), 2476–2492. <https://doi.org/10.1002/2016JG003386>
- Chen, W., Wang, S., Wang, J., Xia, J., Luo, Y., Yu, G., & Niu, S. (2023). Evidence for widespread thermal optimality of ecosystem respiration. *Nature Ecology & Evolution*, 7(9), 1379–1387. <https://doi.org/10.1038/s41559-023-02121-w>
- Chi, Y., Yang, Q., Zhou, L., Shen, R., Zheng, S., Zhang, Z., et al. (2020). Temperature sensitivity in individual components of ecosystem respiration increases along the vertical gradient of leaf-stem-soil in three subtropical forests. *Forests*, 11(2), 140. <https://doi.org/10.3390/f11020140>
- Davidson, E. A., & Janssens, I. A. (2006). Temperature sensitivity of soil carbon decomposition and feedbacks to climate change. *Nature*, 440(7081), 165–173. <https://doi.org/10.1038/nature04514>
- Davidson, E. A., Richardson, A. D., Savage, K. E., & Hollinger, D. Y. (2006). A distinct seasonal pattern of the ratio of soil respiration to total ecosystem respiration in a spruce-dominated forest. *Global Change Biology*, 12(2), 230–239. <https://doi.org/10.1111/j.1365-2486.2005.01062.x>
- Davidson, E. A., Samanta, S., Caramori, S. S., & Savage, K. (2012). The Dual Arrhenius and Michaelis-Menten kinetics model for decomposition of soil organic matter at hourly to seasonal time scales. *Global Change Biology*, 18(1), 371–384. <https://doi.org/10.1111/j.1365-2486.2011.02546.x>

- Drake, J. E., Macdonald, C. A., Tjoelker, M. G., Reich, P. B., Singh, B. K., Anderson, I. C., & Ellsworth, D. S. (2018). Three years of soil respiration in a mature eucalypt woodland exposed to atmospheric CO₂ enrichment. *Biogeochemistry*, *139*(1), 85–101. <https://doi.org/10.1007/s10533-018-0457-7>
- Fanin, N., Mooshammer, M., Sauvadet, M., Meng, C., Alvarez, G., Bernard, L., et al. (2022). Soil enzymes in response to climate warming: Mechanisms and feedbacks. *Functional Ecology*, *36*(6), 1378–1395. <https://doi.org/10.1111/1365-2435.14027>
- Friedlingstein, P., O'Sullivan, M., Jones, M. W., Andrew, R. M., Bakker, D. C. E., Hauck, J., et al. (2023). Global carbon budget 2023. *Earth System Science Data*, *15*(12), 5301–5369. <https://doi.org/10.5194/essd-15-5301-2023>
- Griebel, A., Metzén, D., Boer, M. M., Barton, C. V., Renchon, A. A., Andrews, H. M., & Pendall, E. (2020). Using a paired tower approach and remote sensing to assess carbon sequestration and energy distribution in a heterogeneous sclerophyll forest. *Science of the Total Environment*, *699*, 133918. <https://doi.org/10.1016/j.scitotenv.2019.133918>
- Griffis, T. J., Black, T. A., Gaumont-Guay, D., Drewitt, G. B., Nesic, Z., Barr, A. G., et al. (2004). Seasonal variation and partitioning of ecosystem respiration in a southern boreal aspen forest. *Agricultural and Forest Meteorology*, *125*(3–4), 207–223. <https://doi.org/10.1016/j.agrformet.2004.04.006>
- Guidolotti, G., Rey, A., D'Andrea, E., Matteucci, G., & De Angelis, P. (2013). Effect of environmental variables and stand structure on ecosystem respiration components in a Mediterranean beech forest. *Tree Physiology*, *33*(9), 960–972. <https://doi.org/10.1093/treephys/tpz065>
- Hao, G., Zhuang, Q., Zhu, Q., He, Y., Jin, Z., & Shen, W. (2015). Quantifying microbial ecophysiological effects on the carbon fluxes of forest ecosystems over the conterminous United States. *Climate Change*, *133*(4), 695–708. <https://doi.org/10.1007/s10584-015-1490-3>
- Haverd, V., & Cuntz, M. (2010). Soil–Litter–Iso: A one-dimensional model for coupled transport of heat, water and stable isotopes in soil with a litter layer and root extraction. *Journal of Hydrology*, *388*(3–4), 438–455. <https://doi.org/10.1016/j.jhydrol.2010.05.02>
- Haverd, V., Raupach, M., Briggs, P., Canadell, J., Isaac, P., Pickett-Heaps, C., et al. (2013). Multiple observation types reduce uncertainty in Australia's terrestrial carbon and water cycles. *Biogeosciences*, *10*(3), 2011–2040. <https://doi.org/10.5194/bg-10-2011-2013>
- Haverd, V., Smith, B., Nieradzki, L., Briggs, P. R., Woodgate, W., Trudinger, C. M., et al. (2018). A new version of the CABLE land surface model (Subversion revision r4546), incorporating land use and land cover change, woody vegetation demography and a novel optimisation-based approach to plant coordination of electron transport and carboxylation capacity-limited photosynthesis. *Geoscientific Model Development*, *11*(7), 2995–3026. <https://doi.org/10.5194/gmd-11-2995-2018>
- Hopkins, F., Gonzalez-Meler, M. A., Flower, C. E., Lynch, D. J., Czimeczik, C., Tang, J., & Subke, J. (2013). Ecosystem-level controls on root-rhizosphere respiration. *New Phytologist*, *199*(2), 339–351. <https://doi.org/10.1111/nph.12271>
- IPCC. (2022). In H.-O. Pörtner, D. C. Roberts, M. Tignor, E. S. Poloczanska, K. Mintenbeck, et al. (Eds.), *Climate change 2022: Impacts, adaptation, and vulnerability. Contribution of working group II to the sixth assessment report of the intergovernmental panel on climate change* (p. 3056). Cambridge University Press.
- Isaac, P., Cleverly, J., McHugh, I., van Gorsel, E., Ewenz, C., & Beringer, J. (2017). OzFlux data: Network integration from collection to curation. *Biogeosciences*, *14*(12), 2903–2928. <https://doi.org/10.5194/bg-14-2903-2017>
- Jiang, M., Medlyn, B. E., Drake, J. E., Duursma, R. A., Anderson, I. C., Barton, C. V. M., et al. (2020). The fate of carbon in a mature forest under carbon dioxide enrichment. *Nature*, *580*(7802), 227–231. <https://doi.org/10.1038/s41586-020-2128-9>
- Johnston, A. S. A., Meade, A., Ardö, J., Arriga, N., Black, A., Blanken, P. D., et al. (2021). Temperature thresholds of ecosystem respiration at a global scale. *Nature Ecology & Evolution*, *5*(4), 487–494. <https://doi.org/10.1038/s41559-021-01398-z>
- Khomik, M., Arain, M. A., Brodeur, J. J., Peichl, M., Restrepo-Coupe, N., & McLaren, J. D. (2010). Relative contributions of soil, foliar, and woody tissue respiration to total ecosystem respiration in four pine forests of different ages. *Journal of Geophysical Research*, *115*(G3), G03024. <https://doi.org/10.1029/2009JG001089>
- Law, B. E., Ryan, M. G., & Anthoni, P. M. (1999). Seasonal and annual respiration of a ponderosa pine ecosystem. *Global Change Biology*, *5*(2), 169–182. <https://doi.org/10.1046/j.1365-2486.1999.00214.x>
- Li, J., Pendall, E., Dijkstra, F. A., & Nie, M. (2020). Root effects on the temperature sensitivity of soil respiration depend on climatic condition and ecosystem type. *Soil and Tillage Research*, *199*, 104574. <https://doi.org/10.1016/j.still.2020.104574>
- Li, N., Shao, J., Zhou, G., Zhou, L., Du, Z., & Zhou, X. (2022). Improving estimations of ecosystem respiration with asymmetric daytime and nighttime temperature sensitivity and relative humidity. *Agricultural and Forest Meteorology*, *312*, 108709. <https://doi.org/10.1016/j.agrformet.2021.108709>
- Liang, L. L., Arcus, V. L., Heskell, M. A., O'Sullivan, O. S., Weerasinghe, L. K., Creek, D., et al. (2018). Macromolecular rate theory (MMRT) provides a thermodynamics rationale to underpin the convergent temperature response in plant leaf respiration. *Global Change Biology*, *24*(4), 1538–1547. <https://doi.org/10.1111/gcb.13936>
- Liu, X., Dong, W., Wood, J. D., Wang, Y., Li, X., Zhang, Y., et al. (2022). Aboveground and belowground contributions to ecosystem respiration in a temperate deciduous forest. *Agricultural and Forest Meteorology*, *314*, 108807. <https://doi.org/10.1016/j.agrformet.2022.108807>
- Lombardozzi, D. L., Bonan, G. B., Smith, N. G., Dukes, J. S., & Fisher, R. A. (2015). Temperature acclimation of photosynthesis and respiration: A key uncertainty in the carbon cycle-climate feedback. *Geophysical Research Letters*, *42*(20), 8624–8631. <https://doi.org/10.1002/2015GL065934>
- Loveys, B. R., Atkinson, L. J., Sherlock, D. J., Roberts, R. L., Fitter, A. H., & Atkin, O. K. (2003). Thermal acclimation of leaf and root respiration: An investigation comparing inherently fast- and slow-growing plant species. *Global Change Biology*, *9*(6), 895–910. <https://doi.org/10.1046/j.1365-2486.2003.00611.x>
- Mahecha, M. D., Reichstein, M., Carvalhais, N., Lasslop, G., Lange, H., Seneviratne, S. I., et al. (2010). Global convergence in the temperature sensitivity of respiration at ecosystem level. *Science*, *329*(5993), 838–840. <https://doi.org/10.1126/science.1189587>
- Makita, N., Fujimoto, R., & Tamura, A. (2021). The contribution of roots, mycorrhizal hyphae, and soil free-living microbes to soil respiration and its temperature sensitivity in a larch forest. *Forests*, *12*(10), 1410. <https://doi.org/10.3390/f12101410>
- Matteucci, M., Gruening, C., Ballarin, I. G., Seufert, G., & Cescatti, A. (2015). Components, drivers and temporal dynamics of ecosystem respiration in a Mediterranean pine forest. *Soil Biology and Biochemistry*, *88*, 224–235. <https://doi.org/10.1016/j.soilbio.2015.05.017>
- McCormack, M. L., Guo, D., Iversen, C. M., Chen, W., Eissenstat, D. M., Fernandez, C. W., et al. (2017). Building a better foundation: Improving root-trait measurements to understand and model plant and ecosystem processes. *New Phytologist*, *215*(1), 27–37. <https://doi.org/10.1111/nph.14459>
- Merganičová, K., Merganič, J., Lehtonen, A., Vacchiano, G., Sever, M. Z. O., Augustynczyk, A. L. D., et al. (2019). Forest carbon allocation modelling under climate change. *Tree Physiology*, *39*(12), 1937–1960. <https://doi.org/10.1093/treephys/tpz105>
- Montané, F., Fox, A. M., Arellano, A. F., MacBean, N., Alexander, M. R., Dye, A., et al. (2017). Evaluating the effect of alternative carbon allocation schemes in a land surface model (CLM4.5) on carbon fluxes, pools, and turnover in temperate forests. *Geoscientific Model Development*, *10*(9), 3499–3517. <https://doi.org/10.5194/gmd-10-3499-2017>

- Nickerson, N., Egan, J., & Risk, D. (2013). Iso-FD: A novel method for measuring the isotopic signature of surface flux. *Soil Biology and Biochemistry*, 62, 99–106. <https://doi.org/10.1016/j.soilbio.2013.03.010>
- Niu, B., Zhang, X., Piao, S., Janssens, I. A., Fu, G., He, Y., et al. (2021). Warming homogenizes apparent temperature sensitivity of ecosystem respiration. *Science Advances*, 7(15), eabc7358. <https://doi.org/10.1126/sciadv.abc7358>
- Noh, N. J., Crous, K. Y., Li, J., Choury, Z., Barton, C. V. M., Arndt, S. K., et al. (2020). Does root respiration in Australian rainforest tree seedlings acclimate to experimental warming? *Tree Physiology*, 40(9), 1192–1204. <https://doi.org/10.1093/treephys/tpaa056>
- Noh, N. J., Crous, K. Y., Salomon, R. L., Li, J., Ellsworth, D. S., Barton, C. V. M., et al. (2021). Elevated CO₂ alters the temperature sensitivity of stem CO₂ efflux in a mature eucalypt woodland. *Environmental and Experimental Botany*, 188, 104508. <https://doi.org/10.1016/j.envexpbot.2021.104508>
- Noh, N. J., Kuribayashi, M., Saitoh, T. M., & Muraoka, H. (2017). Different responses of soil, heterotrophic and autotrophic respiration to a 4-year soil warming experiment in a cool-temperate deciduous broadleaved forest in central Japan. *Agricultural and Forest Meteorology*, 247, 560–570. <https://doi.org/10.1016/j.agrformet.2017.09.002>
- Oikawa, P. Y., Sturtevant, C., Knox, S. H., Verfaillie, J., Huang, Y. W., & Baldocchi, D. D. (2017). Revisiting the partitioning of net ecosystem exchange of CO₂ into photosynthesis and respiration with simultaneous flux measurements of ¹³CO₂ and CO₂, soil respiration and a biophysical model, CANVEG. *Agricultural and Forest Meteorology*, 234–235, 149–163. <https://doi.org/10.1016/j.agrformet.2016.12.016>
- Ouimette, A. P., Ollinger, S. V., Richardson, A. D., Hollinger, D. Y., Keenan, T. F., Lepine, L. C., & Vadeboncoeur, M. A. (2018). Carbon fluxes and interannual drivers in a temperate forest ecosystem assessed through comparison of top-down and bottom-up approaches. *Agricultural and Forest Meteorology*, 256–257, 420–430. <https://doi.org/10.1016/j.agrformet.2018.03.017>
- Pendall, E., & Noh, N. J. (2024). Noh_rawdata_v20240214.xlsx [Dataset]. [figshare](https://doi.org/10.6084/m9.figshare.25246198.v1). <https://doi.org/10.6084/m9.figshare.25246198.v1>
- Phillips, C. L., Bond-Lamberty, B., Desai, A. R., Lavoie, M., Risk, D., Tang, J., et al. (2017). The value of soil respiration measurements for interpreting and modeling terrestrial carbon cycling. *Plant and Soil*, 413(1–2), 1–25. <https://doi.org/10.1007/s11104-016-3084-x>
- Piñeiro, J., Ochoa-Heuso, R., Drake, J. E., Tjoelker, M. G., & Power, S. A. (2020). Water availability drives fine root dynamics in a *Eucalyptus* woodland under elevated atmospheric CO₂ concentration. *Functional Ecology*, 34, 2219–2422. <https://doi.org/10.1111/1365-2435.13660>
- Qubaja, R., Tatarinov, F., Rotenberg, E., & Yakir, D. (2020). Partitioning of canopy and soil CO₂ fluxes in a pine forest at the dry timberline across a 13-year observation period. *Biogeosciences*, 17(3), 699–714. <https://doi.org/10.5194/bg-17-699-2020>
- R Core Team. (2020). *R: A language and environment for statistical computing*. R Foundation for Statistical Computing.
- Renchon, A. A. (2019). *Constraints on ecosystem carbon and water flux estimates in a temperate Australian evergreen forest*. Ph. D. Dissertation (p. 197). Western Sydney University.
- Renchon, A. A., Drake, J. E., Macdonald, C. A., Sihi, D., Hinko-Najera, N., Tjoelker, M. G., et al. (2021). Concurrent measurements of soil and ecosystem respiration in a mature eucalypt woodland: Advantages, lessons, and questions. *Journal of Geophysical Research: Biogeosciences*, 126(3). <https://doi.org/10.1029/2020JG006221>
- Renchon, A. A., Griebel, A., Metzen, D., Williams, C. A., Medlyn, B., Duursma, R. A., et al. (2018). Upside-down fluxes down under: CO₂ net sink in winter and net source in summer in a temperate evergreen broadleaf forest. *Biogeosciences*, 15(12), 3703–3716. <https://doi.org/10.5194/bg-15-3703-2018>
- Renchon, A. A., Haverd, V., Trudinger, C. M., Medlyn, B. E., Griebel, A., Metzen, D., et al. (2024). Temporal dynamics of canopy properties and carbon and water fluxes in a temperate evergreen angiosperm forest. *Forests*, 15(5), 801. <https://doi.org/10.3390/f15050801>
- Risk, D., Nickerson, N., Creelman, C., McArthur, G., & Owens, J. (2011). Forced diffusion soil flux: A new technique for continuous monitoring of soil gas efflux. *Agricultural and Forest Meteorology*, 151(12), 1622–1631. <https://doi.org/10.1016/j.agrformet.2011.06.020>
- Rodríguez-Calcerrada, J., Martin-StPaul, N. K., Lempereur, M., Ourcival, J.-M., del Rey, M. C., Joffre, R., & Rambal, S. (2014). Stem CO₂ efflux and its contribution to ecosystem CO₂ efflux decrease with drought in a Mediterranean forest stand. *Agricultural and Forest Meteorology*, 195–196, 61–72. <https://doi.org/10.1016/j.agrformet.2014.04.012>
- Salomón, R. L., De Roo, L., Oleksyn, J., De Pauw, D. J. W., & Steppe, K. (2020). TReSpire—A biophysical tree stem respiration model. *New Phytologist*, 225(5), 2214–2230. <https://doi.org/10.1111/nph.16174>
- Savage, K. E., Davidson, E. A., Abramoff, R. Z., Finzi, A. C., & Giasson, M.-A. (2018). Partitioning soil respiration: Quantifying the artifacts of the trenching method. *Biogeochemistry*, 140(1), 53–63. <https://doi.org/10.1007/s10533-018-0472-8>
- Sihi, D., Davidson, E. A., Chen, M., Savage, K. E., Richardson, A. D., Keenan, T. F., & Hollinger, D. Y. (2018). Merging a mechanistic enzymatic model of soil heterotrophic respiration into an ecosystem model in two AmeriFlux sites of northeastern USA. *Agricultural and Forest Meteorology*, 252, 155–166. <https://doi.org/10.1016/j.agrformet.2018.01.026>
- Speckman, H. N., Frank, J. M., Bradford, J. B., Miles, B. L., Massman, W. J., Parton, W. J., & Ryan, M. G. (2015). Forest ecosystem respiration estimated from eddy covariance and chamber measurements under high turbulence and substantial tree mortality from bark beetles. *Global Change Biology*, 21(2), 708–721. <https://doi.org/10.1111/gcb.12731>
- Sun, W., Luo, X., Fang, Y., Shiga, Y. P., Zhang, Y., Fisher, J. B., et al. (2023). Biome-scale temperature sensitivity of ecosystem respiration revealed by atmospheric CO₂ observations. *Nature Ecology & Evolution*, 7(8), 1199–1210. <https://doi.org/10.1038/s41559-023-02093-x>
- Tarvainen, L., Rantfors, M., & Wallin, G. (2014). Vertical gradients and seasonal variation in stem CO₂ efflux within a Norway spruce stand. *Tree Physiology*, 34(5), 488–502. <https://doi.org/10.1093/treephys/tpu036>
- Tjoelker, M. G., Oleksyn, J., Lorenc-Plucinska, G., & Reich, P. B. (2009). Acclimation of respiratory temperature responses in northern and southern populations of *Pinus banksiana*. *New Phytologist*, 181(1), 218–229. <https://doi.org/10.1111/j.1469-8137.2008.02624.x>
- Tramontana, G., Migliavacca, M., Jung, M., Reichstein, M., Keenan, T. F., Camps-Valls, G., et al. (2020). Partitioning net carbon dioxide fluxes into photosynthesis and respiration using neural networks. *Global Change Biology*, 26(9), 5235–5253. <https://doi.org/10.1111/gcb.15203>
- Trumbore, S. (2006). Carbon respired by terrestrial ecosystems—Recent progress and challenges. *Global Change Biology*, 12(2), 141–153. <https://doi.org/10.1111/j.1365-2486.2006.01067.x>
- Turnbull, M. H., Whitehead, D., Tissue, D. T., Schuster, W. S. F., Brown, K. J., & Griffin, K. L. (2003). Scaling foliar respiration in two contrasting forest canopies. *Functional Ecology*, 17(1), 101–114. <https://doi.org/10.1046/j.1365-2435.2003.00713.x>
- Vargas, R., & Allen, M. F. (2008). Environmental controls and the influence of vegetation type, fine roots and rhizomorphs on diel and seasonal variation in soil respiration. *New Phytologist*, 179(2), 460–471. <https://doi.org/10.1111/j.1469-8137.2008.02481.x>
- Walker, A. P., Beckerman, A. P., Gu, L., Kattge, J., Cernusak, L. A., Domingues, T. F., et al. (2014). The relationship of leaf photosynthetic traits—V_{max} and J_{max}—to leaf nitrogen, leaf phosphorus, and specific leaf area: A meta-analysis and modeling study. *Ecology and Evolution*, 4(16), 3218–3235. <https://doi.org/10.1002/ece3.1173>
- Wang, W., Wang, H., Zu, Y., Li, X., & Koike, T. (2006). Characteristics of the temperature coefficient, Q₁₀, for the respiration of non-photosynthetic organs and soils of forest ecosystems. *Frontiers of Forestry in China*, 2, 125–135. <https://doi.org/10.1007/s11461-006-0018-4>

- Wang, X., Liu, L., Piao, S., Janssens, I. A., Tang, J., Liu, W., et al. (2014). Soil respiration under climate warming: Differential response of heterotrophic and autotrophic respiration. *Global Change Biology*, *20*(10), 3229–3237. <https://doi.org/10.1111/gcb.12620>
- Wang, X., Wang, C., & Bond-Lamberty, B. (2017). Quantifying and reducing the differences in forest CO₂-fluxes estimated by eddy covariance, biometric and chamber methods: A global synthesis. *Agricultural and Forest Meteorology*, *247*, 93–103. <https://doi.org/10.1016/j.agrformet.2017.07.023>
- Wang, Y. P., Law, R. M., & Pak, B. (2010). A global model of carbon, nitrogen and phosphorus cycles for the terrestrial biosphere. *Biogeosciences*, *7*, 2261–2282. <https://doi.org/10.5194/bg-7-2261-2010>
- Wang, Y.-P., & Leuning, R. (1998). A two-leaf model for canopy conductance, photosynthesis and partitioning of available energy I: Model description and comparison with a multi-layered model. *Agricultural and Forest Meteorology*, *91*(1–2), 89–111. [https://doi.org/10.1016/S0168-1923\(98\)00061-6](https://doi.org/10.1016/S0168-1923(98)00061-6)
- Warren, J. M., Hanson, P. J., Iversen, C. M., Kumar, J., Walker, A. P., & Wullschlegel, S. D. (2015). Root structural and functional dynamics in terrestrial biosphere models—Evaluation and recommendations. *New Phytologist*, *205*(1), 59–78. <https://doi.org/10.1111/nph.13034>
- Wohlfahrt, G., & Galvagno, M. (2017). Revisiting the choice of the driving temperature for eddy covariance CO₂ flux partitioning. *Agricultural and Forest Meteorology*, *237*, 135–142. <https://doi.org/10.1016/j.agrformet.2017.02.012>
- Yang, J., Medlyn, B. E., De Kauwe, M. G., Duursma, R. A., Jiang, M., Kumarathunge, D., et al. (2020). Low sensitivity of gross primary production to elevated CO₂ in a mature eucalypt woodland. *Biogeosciences*, *17*(2), 265–279. <https://doi.org/10.5194/bg-17-265-2020>
- Yao, Y. T., Ciais, P., Viogy, N., Li, W., Cresto-Aleina, F., Yang, H., et al. (2021). A data-driven global soil heterotrophic respiration dataset and the drivers of its inter-annual variability. *Global Biogeochemical Cycles*, *35*(8), e2020GB006918. <https://doi.org/10.1029/2020GB006918>
- Yuan, J., Jose, S., Hu, Z., Pang, J., Hou, L., & Zhang, S. (2018). Biometric and eddy covariance methods for examining the carbon balance of a *Larix principis-rupprechtii* forest in the Qinling Mountains, China. *Forests*, *9*(2), 67. <https://doi.org/10.3390/f9020067>
- Zhang, Z., Zhang, H., Cui, Z., Tao, F., Chen, Z., Chang, Y., et al. (2021). Global consistency in response of terrestrial ecosystem respiration to temperature. *Agricultural and Forest Meteorology*, *308–309*, 108576. <https://doi.org/10.1016/j.agrformet.2021.108576>
- Zhao, K., Dong, B., Jia, Z., & Ma, L. (2018). Effect of climatic factors on the temporal variation of stem respiration in *Larix principis-rupprechtii* Mayr. *Agricultural and Forest Meteorology*, *248*, 441–448. <https://doi.org/10.1016/j.agrformet.2017.10.033>